Available online at www.sciencedirect.com
SCIENCE DIRECT®

Polymer 47 (2006) 1318–1323

polymer

www.elsevier.com/locate/polymer

Electrical and optical properties of a polyblend electrolyte

Ch.V. Subba Reddy *, A.K. Sharma, V.V.R. Narasimha Rao

Department of Physics, S.V. University, Tirupati 517 502, India

Received 8 June 2005; received in revised form 31 October 2005; accepted 11 December 2005
Available online 18 January 2006

Abstract

A potassium ion conducting polyblend electrolyte based on polyvinyl pyrrolidone (PVP)+polyvinyl alcohol (PVA) complexed with $KBrO_3$ was prepared using solution cast technique. The electrical conductivity increased with increasing dopant concentration. Optical absorption studies were made in the wavelength range (200–600 nm) on pure (PVP+PVA) and $KBrO_3$ doped (PVP+PVA) films. The absorption edge was observed at 5.13 eV for undoped (PVP+PVA) while it ranged from 4.88 to 5.0 eV for differently $KBrO_3$-doped samples. The direct band gaps for undoped and $KBrO_3$ doped (PVP+PVA) films were found to be, respectively, 5.05 and 4.95, 4.86 and 4.90 eV while the indirect band gaps were 5.03 and 4.88, 4.79 and 4.83 eV, respectively. The absorption edge and the band gaps moved towards lower energies as the dopant concentration was increased up to 20 wt% of the dopant. For further increase in dopant concentration these values started increasing again. This is explained in terms of formation of charge transfer complexes between the dopant and the host matrix. The thermal properties of these films were investigated with differential scanning calorimetry (DSC). The variation in film morphology is examined by scanning electron microscopic examination.

Keywords: Absorption edge; Optical band gaps; Glass transition temperature (T_g)

1. Introduction

In recent years, studies on the electrical and optical properties of polymers have attracted much attention in view of their application in electronic and optical devices. Electrical conduction in polymers has been studied aiming to understand the nature of the charge transport prevalent in these materials while the optical properties are aimed at achieving better reflection, antireflection, interference and polarization properties. The electrical and optical properties of polymers can be suitably modified by the addition of dopants depending on their reactivity with the host matrix. Although some work has been reported on the charge carrier transport and optical properties of doped polymers [1–7], very little work is available on doped polyblend of (PVP+PVA) films [8,9]. (PVP+PVA) is a potential material having a very high dielectric strength, good charge storage capacity and dopant-dependent electrical and optical properties. Since K^+ is a fast conducting ion in a number of crystalline and amorphous materials, its incorporation in a polymeric system may be expected to enhance its electrical and optical performance. This paper presents the results of such investigations on the electrical and optical properties of $KBrO_3$-doped (PVP+PVA) films.

2. Experimental

Films (thickness ~ 150 μm) of pure blends of (PVP+PVA) and various compositions of complexed films of (PVP+PVA) with a salt of $KBrO_3$ were prepared in the weight percent ratios (45:45:10), (40:40:20) and (35:35:30) by solution cast technique using triple distilled water as a solvent. The solutions were stirred for 10–12 h and then cast on to polypropylene dishes and evaporated slowly at room temperature. The final product was vacuum dried thoroughly at 0.13 pa.

For the DSC measurements a Netzsch DSC 200, operating in dynamic mode (heating rate = 10 K/min), was employed. Samples of ≈ 5 mg weight were placed in sealed aluminium pans. Prior to use the calorimeter was calibrated with metal standards; an empty aluminium pan being used as a reference. The morphology of the samples was characterized by an JSM-5610LV scanning electron microscope (SEM).

The DC conductivities were measured using an in-house instrument [10], in the temperature range 300–427 K. Optical absorption spectra were recorded at room temperature in the wavelength region 200–600 nm using Shimadzu UV–VIS-NIR (Model UV-3100) spectrophotometer. From these data the optical constants such as band edge, optical band gap (both direct and indirect) were determined.

---

* Corresponding author. Tel.: +91 8772249273; fax: +91 8772248499.
E-mail address: drsreddy2005@yahoo.com (C.V. Subba Reddy).

0032-3861/$ - see front matter
doi:10.1016/j.polymer.2005.12.052

3. Results and discussion

The variation of DC conductivity, σ, as a function of composition of $KBrO_3$ in (PVP+PVA) for different weight percent ratios is shown in Fig. 1 for films prepared at different temperatures.

The conductivity of pure (PVP+PVA) was 4.61×10^{-7} S/cm at room temperature and its value increased about 10 times on complexing it with 10% $KBrO_3$. As the rise of conductivity is significant with increased concentration of $KBrO_3$.

The increase in conductivity with increasing concentration of $KBrO_3$ is attributed to the decrease in the degree of crystallinity and increase in the degree of amorphosity [8]. In amorphous regions, the chains are irregular and entangled where as in crystalline regions the chains are regularly arranged. Hence, it is very easy to move the molecular chains in the amorphous state rather than the crystalline state. The molecular packing in the amorphous state is weak and so the density is smaller than that of crystalline regions. Thus the chains in the amorphous phase are more flexible and are capable of orienting themselves relatively more easily and rapidly.

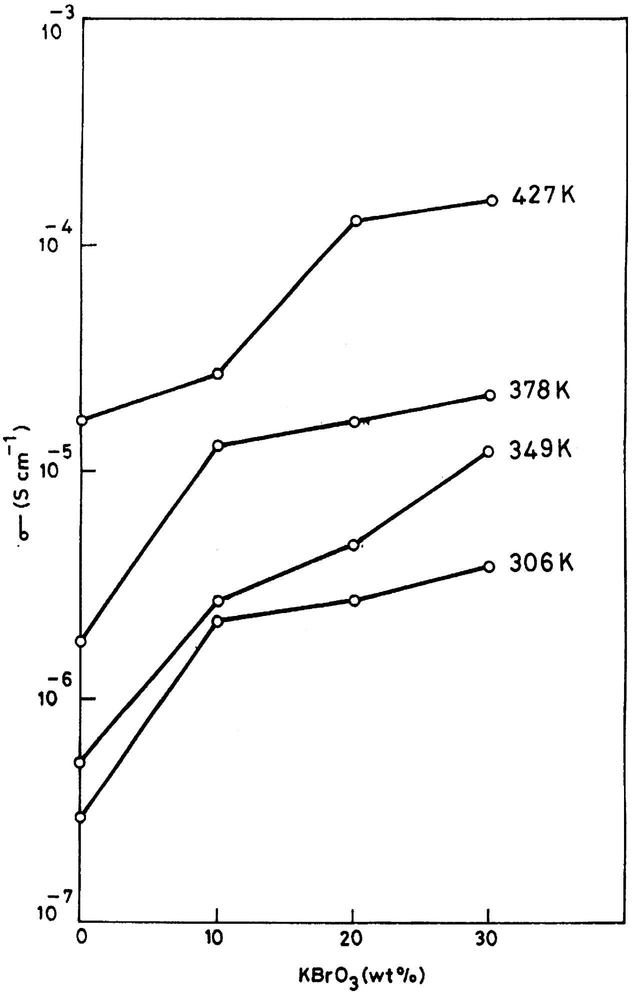

Fig. 1. Composition vs conductivity plots of (PVP+PVA+$KBrO_3$ polyblend electrolyte system at different temperature.

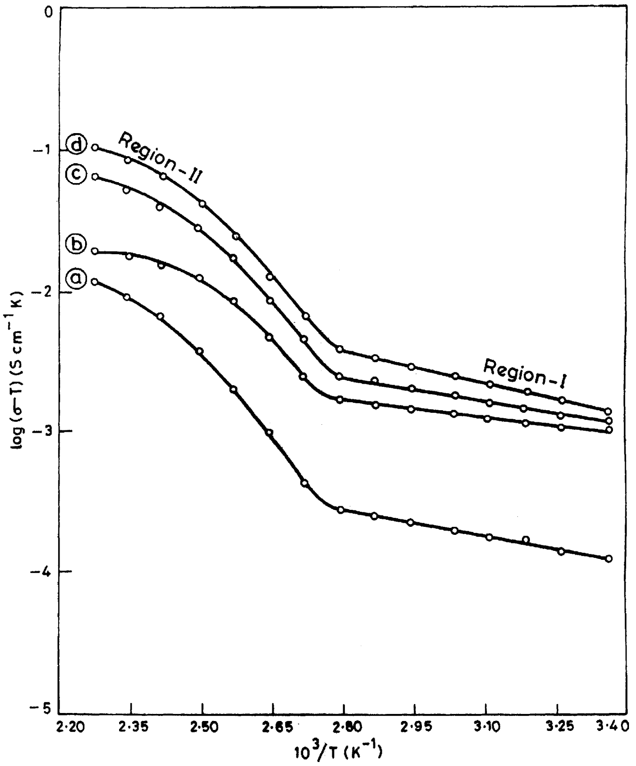

Fig. 2. Temperature dependent conductivity of (a) pure (PVP+PVA) (50:50); (b) (PVP+PVA+$KBrO_3$) (45:45:10); (c) (PVP+PVA+$KBrO_3$) (40:40:20); (d) (PVP+PVA+$KBrO_3$) (35:35:30).

Fig. 2 shows the variation of DC electrical conductivity as function of temperature for pure (PVP+PVA) and for different compositions of (PVP+PVA+$KBrO_3$) polyblend electrolyte in the temperature range of 300–427 K. The following sailent features were noticed:

(i) In the temperature range of study, the conductivity is found to increase with increase of temperature in pure (PVP+PVA) as well as in all the compositions of (PVP+PVA+$KBrO_3$) polyblend electrolyte.
(ii) From Fig. 2 it is clear that, the conductivity–temperature plots follow Arrehenius behaviour throughout with two regions of different activation energies.

The existence of two regions (region I and II) in the conductivity vs. temperature plots and the sudden increase in the conductivity may be attributed to the transition from semi-crystalline phase to amorphous phase, which is confirmed from DSC studies. Due to this phase change, the conductivity shows a sudden increase. Similar behaviour has been reported on polyvinyl chloride [11], polycrystalline *p*-terphenyl [12], poly(acrylic acid) [13], poly(vinyl alcohol) based electrolyte films [14–18] and PEO based polymer electrolyte films [19–29].

The variation of electrical conductivity (σ) as a function of temperature (T) in the entire temperature range can be fitted to

Table 1
Activation energies (E_a) of (PVP+PVA+$KBrO_3$) polyblend electrolyte system

Polyblend electrolyte system (wt%)	Region I (eV)	Region II (eV)
(PVP+PVA) (50:50)	0.19	0.49
(PVP+PVA+$KBrO_3$) (45:45:10)	0.12	0.33
(PVP+PVA+$KBrO_3$) (40:40:20)	0.13	0.37
(PVP+PVA+$KBrO_3$) (35:35:30)	0.17	0.43

the relation [30],

$$\sigma = \sigma_0 \exp\left(\frac{-E_a}{kT}\right)$$

where σ_0 is a constant, k, the Boltzmann constant and E_a, the activation energy.

The calculated activation energies (E_a) in the two regions for (PVP+PVA+$KBrO_3$) complexes are summarised in Table 1.

The activation energies calculated from the slopes of $\log(\sigma T)$ V_s $1/T$ plots in both regions show a decrease in their value with increasing dopant concentration up to 10 wt% of $KBrO_3$ and then an increase with further increase in dopant concentration.

The decrease in activation energies on doping up to 10 wt % of $KBrO_3$ may be explained on the basis of the fact that the incorporation of small amounts of the dopant forms charge transfer complexes in the host lattice [31]. These charge transfer complexes increase the electrical conductivity by providing additional charges in the lattice. This results in a decrease of activation energy. But when the dopant concentration increases further, it leads to segregation of the dopant in the host matrix, which is confirmed from SEM photographs. This segregation impedes the motion of charge carriers resulting in decreased conductivity and hence increased activation energy.

In the region I activation energy due to hopping mechanism between coordinating sites, local structural relaxations and segmental motions of the polymer blends in semi crystalline phase. In the region II activation due to as amorphous regions progressively increase, however, the polymer chain acquires faster internal modes in which bond rotations produce segmental motion.

The study of optical absorption gives information about the band structure of solids. Insulators/semiconductors are generally classified into two types; (a) direct band gap and (b) indirect band gap. In direct band gap semiconductors, the top of the valance band and the bottom of the conduction band both lie at same zero crystal momentum (wave vector). If the bottom of the conduction band does not correspond to zero crystal momentum, then it is called indirect band gap semiconductor. In indirect band gap materials transition from valence to conduction band should always be associated with a phonon of the right magnitude of crystal momentum. Davis and Shalliday [32] reported that near the fundamental band edge, both direct and indirect transitions occur and can be observed by plotting $\alpha^{1/2}$ and α^2 as a function of energy ($h\nu$). The analysis of Thutpalli and Tomlin [33] is based on the following relations:

$$(h\nu n\alpha)^2 = C_1(h\nu - E_{gd})$$

$$(h\nu n\alpha)^{1/2} = C_2(h\nu - E_{gi})$$

where $h\nu$ is the photon energy, E_{gd}, the direct band gap, E_{gi}, the indirect band gap, n, the refractive index, α, the absorption coefficient and C_1, C_2 are constants.

These expressions can be applied to both direct and indirect transitions and are helpful in the determination of the band structure of materials.

When a direct band gap exists, the absorption coefficient has the following dependence on the energy of the incident photon [32,33],

$$\alpha h\nu = C(h\nu - E_g)^{1/2}$$

where E_g is the band gap, C, is a constant dependent on the specimen structure, α is the absorption coefficient, ν is the frequency of the incident light, and h, the Planck's constant.

To determine the nature and width of the band gap, α, $(\alpha h\nu)^2$, $(\alpha h\nu)^{1/2}$ were plotted as a function of photon energy

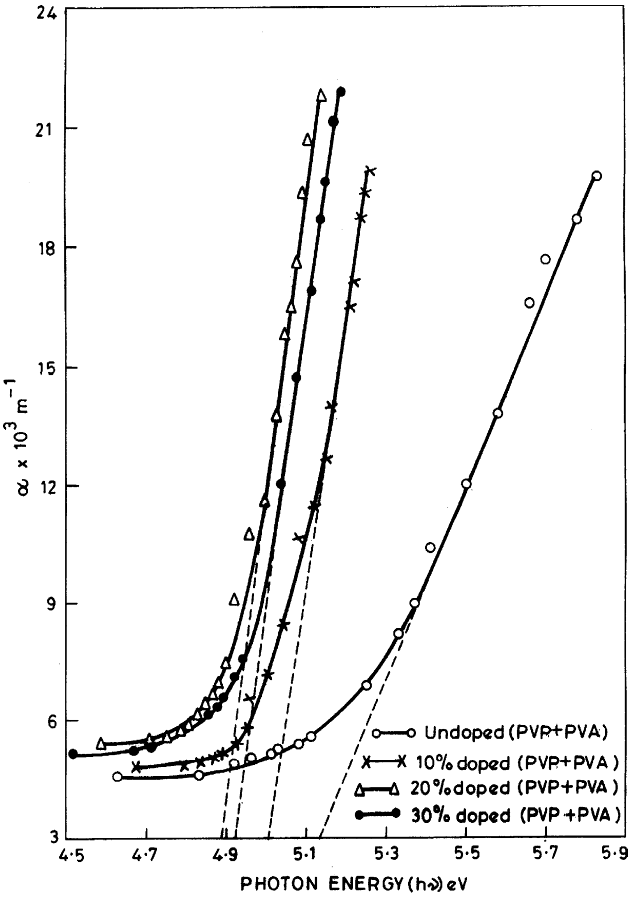

Fig. 3. α vs $h\nu$ (Photon energy) plots of undoped polyblend of (PVP+PVA) and $KBrO_3$ doped (PVP+PVA) films.

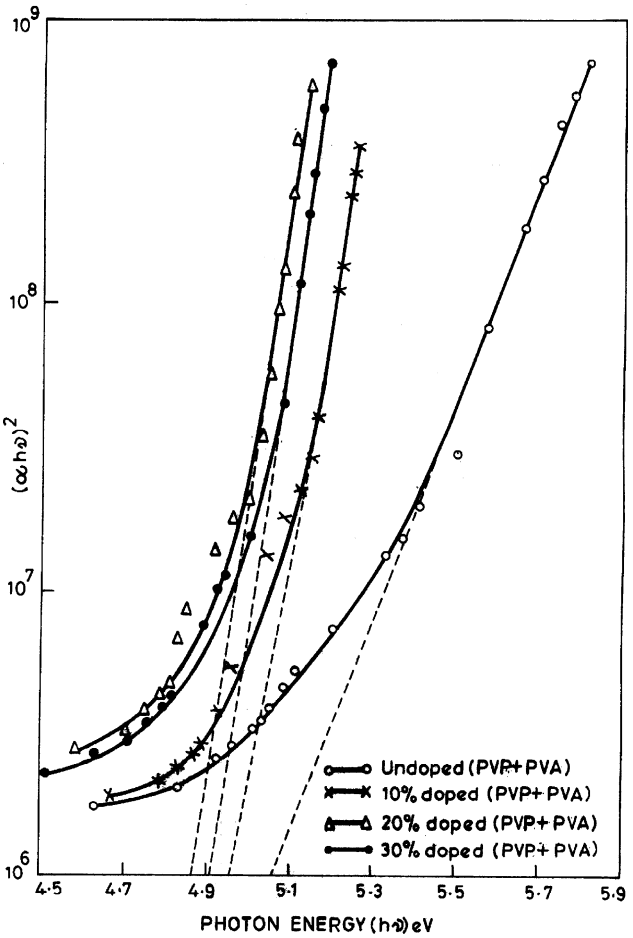

Fig. 4. $(\alpha h\nu)^2$ vs $h\nu$ (Photon energy) plots of undoped polyblend of (PVP+PVA) and $KBrO_3$ doped (PVP+PVA) films.

($h\nu$) (Figs. 3–5) and the absorption edge values were obtained by extrapolating the linear portions of the curves to zero absorption value. It was observed that the absorption edge for pure (PVP+PVA) polyblend film lies at 5.13 eV whereas for 10, 20 and 30 wt% $KBrO_3$ doped (PVP+PVA) polyblend films the absorption edge lies at 5.0, 4.88 and 4.92 eV, respectively (Fig. 3).

The optical band gaps were evaluated from $(\alpha h\nu)^2$ vs $h\nu$ (photon energy) plots and the allowed direct transition energies were determined by extrapolating the linear portion of the curves to zero absorption. For pure (PVP+PVA) polyblend electrolyte the direct band gap lies at 5.05 eV while for 10 and 20, 30 wt% $KBrO_3$ doped (PVP+PVA) electrolyte, it lies at 4.95 and 4.86, 4.90 eV, respectively (Fig. 4).

For indirect transitions, which require photon assistance, the absorption coefficient has the following dependence on the photon energy [32,33].

$$\alpha h\nu = A[h\nu - E_g + E_p]^2 + B[h\nu - E_g - E_p]^2$$

where E_p is the energy of the photon associated with the transition and A and B are constants depending on the band structure.

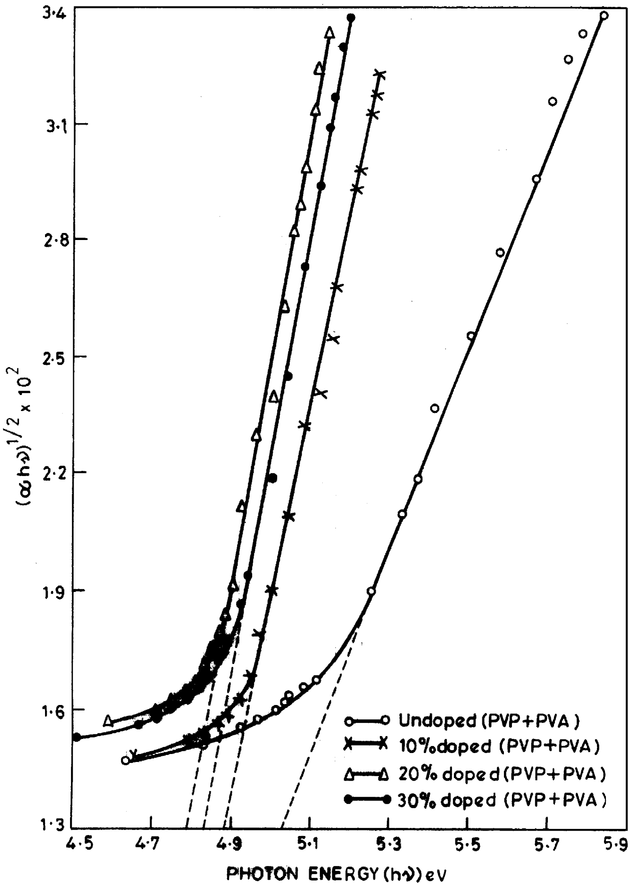

Fig. 5. $(\alpha h\nu)^{1/2}$ vs $h\nu$ (Photon energy) plots of undoped polyblend of (PVP+PVA) and $KBrO_3$ doped (PVP+PVA) films.

The indirect band gaps were obtained from the plots of $(\alpha h\nu)^{1/2}$ vs $h\nu$ (photon energy) plots as shown in Fig. 5. For pure (PVP+PVA) polyblend electrolyte the indirect band gap lies at 5.03 eV while for 10, 20 and 30 wt% $KBrO_3$ doped (PVP+PVA) electrolytes, it lies at 4.88, 4.79 and 4.83 eV, respectively. These values are tabulated in Table 2 together with the absorption edge values, the direct band gap energies and the activation energies obtained from conductivity measurements.

The band edge, direct band gap and indirect band gap values shifted to higher energies on doping with $KBrO_3$ up

Table 2
Absorption edge, optical band gap (both direct and indirect) and activation energy values of undoped and $KBrO_3$ doped (PVP+PVA) polyblend films

Polyblend electrolyte (wt%)	Absorption edge (eV)	Band gap (eV)		Activation energy (eV)	
		Direct	Indirect	Region I	Region II
Undoped (PVP+PVA) (50:50)	5.13	5.05	5.03	0.19	0.49
(PVP+PVA+$KBrO_3$) (45:45:10)	5.00	4.95	4.88	0.12	0.33
(PVP+PVA+$KBrO_3$) (40:40:20)	4.88	4.86	4.79	0.13	0.37
(PVP+PVA+$KBrO_3$) (35:35:30)	4.92	4.90	4.83	0.17	0.43

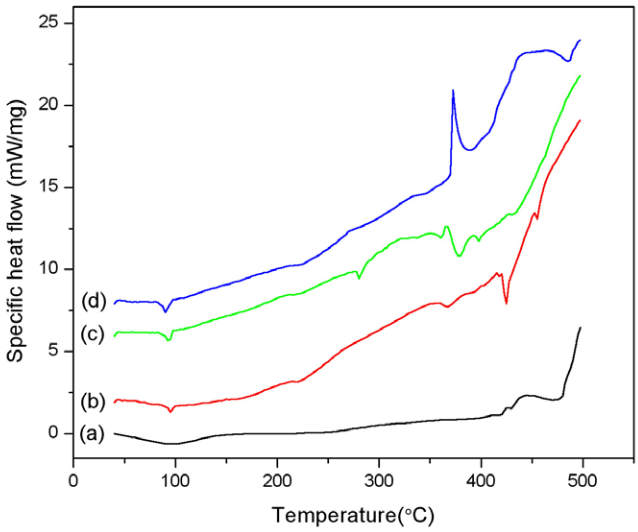

Fig. 6. DSC curves of (a) pure (PVP+PVA). (b) (PVP+PVA+$KBrO_3$) (90:10). (c) (PVP+PVA+$KBrO_3$) (80:20). (d) (PVP+PVA+$KBrO_3$) (70:30).

to a dopant concentration of 10 wt%. For further increase in dopant concentration these shifted to lower energies. The wide variation in the magnitudes of the optical band gap vis-a-vis the activation energies may be attributed to the fact that their nature is different. While the activation energy corresponds to the energy required for conduction from one site to another, the optical band gap corresponds to inter band transition [7].

Fig. 6 shows DSC analyses of the pure (PVP+PVA) and for different compositions of (PVP+PVA+$KBrO_3$) polyblend electrolyte in the temperature range of 40–500 °C. The one observed $T_g^{'}$s are in the following order: pure (PVP+PVA) (96.4 °C) < 10 wt% doped $KBrO_3$ (95.12 °C) < 20 wt% doped $KBrO_3$ (92.62 °C) < 30 wt% doped $KBrO_3$ (90.12 °C) and another $T_g^{'}$s are observed in the region of 350–450 °C at these $T_g^{'}$s a phase change is acquire from semi crystalline to amorphous. Two T_g values have been observed [34] for interpenetrating polymer networks (IPNs), which are multi-phase systems with a complex morphology. The same observations were made for blends having large domain sizes of 10–50 nm [35]. A single T_g is not a measure of miscibility (as defined in classical thermodynamic terms), but only of the state of dispersion [36]. The significant T_g decreases with increasing dopant concentration may be the reduced dipole interactions in its homopolymers. The morphology of the pure (PVP+PVA) and (PVP+PVA+$KBrO_3$) (90:10); (80:20); (70:30) polymer electrolytes, studied by the SEM technique, is of a uniform type, but with differing degrees of roughness (Fig. 7(a)–(d)). Which suggest that the PVP molecules may

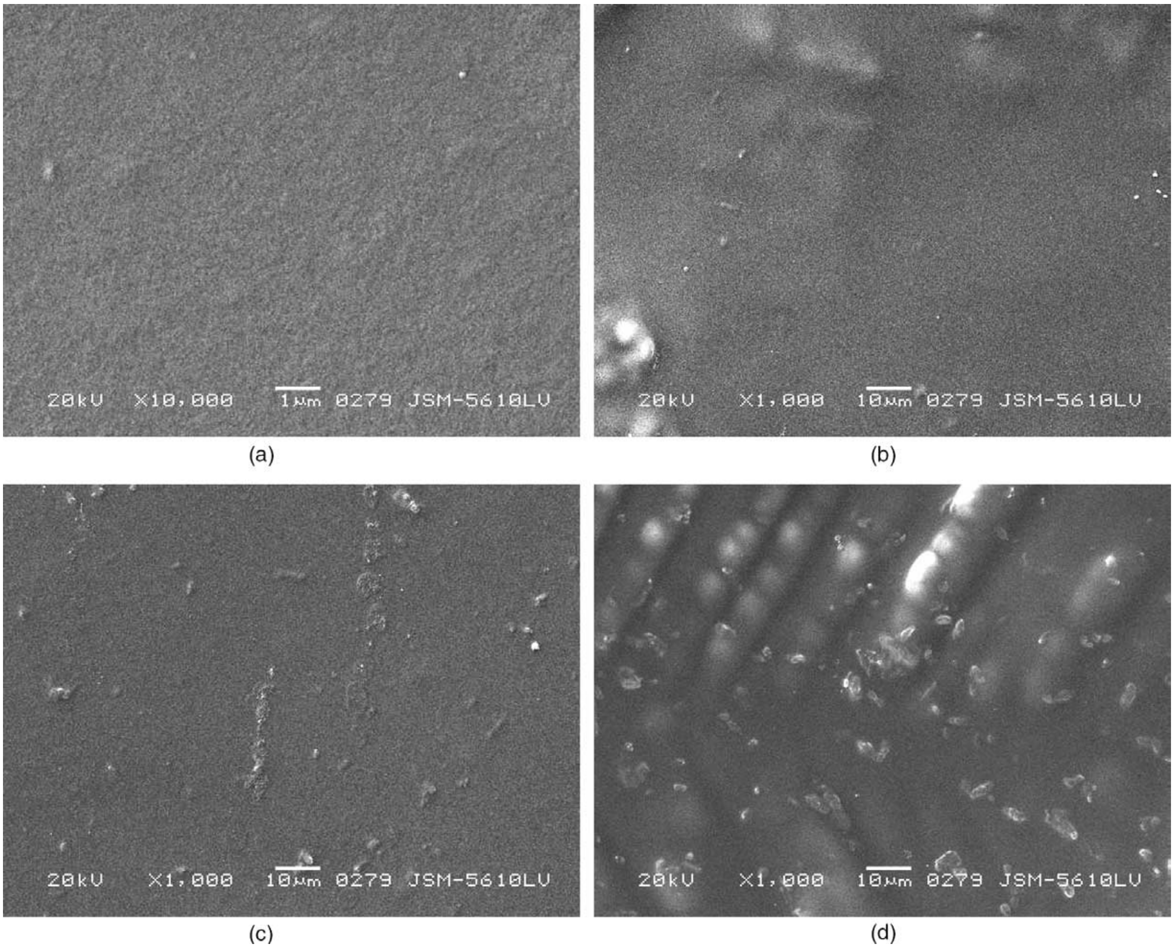

(a) (b) (c) (d)

Fig. 7. SEM photo graphs of (a) pure (PVP+PVA). (b) (PVP+PVA+$KBrO_3$) (90:10). (c) (PVP+PVA+$KBrO_3$) (80:20). (d) (PVP+PVA+$KBrO_3$) (70:30).

disperse in the soft-segment phase with little influence on the microphase separation and mixing of the hard and soft segments. The increase of the degree of roughness with increased $KBrO_3$ concentration indicates segregation of the dopant in the host matrix.

4. Conclusions

The increase in conductivity with increasing concentration of $KBrO_3$ is attributed to the decrease in the degree of crystallinity and increase in the degree of amorphosity. The calculated activation energies in both regions show a decrease in their value with increasing dopant concentration up to 10 wt% of $KBrO_3$ and then an increase with further increase in dopant concentration. Optical absorption edge and optical energy gap (both direct and indirect) showed decreasing trend with increased concentration. Thermal characteristics of pure (PVP + PVA) and for different compositions of (PVP + PVA + $KBrO_3$) polyblend electrolyte have been assessed by thermal analysis method. The significant T_g decreases with increasing dopant concentration may be the reduced dipole interactions in its homopolymers.

Acknowledgements

One of the authors (Ch.V.S. Reddy) wishes to thank the CSIR, New Delhi for the financial support in the form of Senior Research Fellowship to carry out the above work.

References

[1] Ulanski J, Polanowski P, Traiez A, Hofmann M, Dormann E, Laukhina E. Synth Met 1998;94:23.
[2] Chen X, Deng WG, Chen Q. Solid State Commun 1997;103:259.
[3] Aleshin AN, Mironkov NB, Suvarov AV, Conklin JA, SU JM, Kaner RB. Phys Rev B: Condens Matter 1996;54:11638.
[4] Onoda M, Manada Y, Morita S, Yoshino K. J Phys Soc Jpn 1989;58:1895.
[5] Sharma AK, Ramu CH. J Mater Sci Lett 1991;10:1217.
[6] Pruneanu S, Turch R, Brie M, Mihailesan G. Mater Sci Forum 1995; 191:241.
[7] Uma Devi C, Sharma AK, Rao VVRN. Mater Lett 2002;56:167.
[8] Subba Reddy ChV, Sharma AK, Narasimha Rao VVR. J Mater Sci Lett 2002;21:105.
[9] Subba Reddy ChV, Sharma AK, Narasimha Rao VVR. J Power Sources 2002;111:357.
[10] Lakshmi Narayana K. PhD Thesis. SV University; 1995.
[11] Staryga E, Swiatek J. Thin Solid Films 1979;56:311.
[12] Bahri R, Singh HP. Thin Solid Films 1980;69:281.
[13] Narasimha Rao VVR, Mahendar T, Subba Rao B. J Non-Cryst Solids 1988;104:224.
[14] Shukla PK, Agrawal SL. Bull Electrochem 1996;11:732.
[15] Agrawal SL, Shukla PK. Ind J Pure Appl Phys 2000;38:53.
[16] Gupta PN, Singh KP. Solid State Ionics 1996;86:319.
[17] Every HA, Zhou F, Forsyth M, Max farlane DR. Electrochem Acta 1998; 43:1465.
[18] Chandrasekaran R, Mangani IR, Vasanthi R, Selladurai S. Bull Electrochem 2001;17:249.
[19] Huq R, Farrington GC. Solid State Ionics 1988;28:990.
[20] Armand M, Chabagno JM, Duclot M. In: Vashista P, Mudy JN, Shenoy G, editors. Fast ion transport in solids. New York: North Holland; 1979. p. 131.
[21] Steele BCH, Weston SE. Solid State Ionics 1981;2:347.
[22] Bonino F, Scrosati B. In: Chowdari BVR, Radhakrishna S, editors. Polymeric electrolytes in materials for solid state batteries. Singapore: World Scientific; 1986. p. 42.
[23] Hashmi SA, Chandra S. Mater Sci Eng B 1995;24:18.
[24] Sreepathi Rao S, Jaipal Reddy M, Laxminarasaiah E, SubbaRao UV. Mater Sci Eng B 1995;33:173.
[25] Maurya KK, Srivastava N, Hashmi SA, Chandra S. J Mater Sci 1992;27: 6357.
[26] Maurya KK, Hashmi SA, Chandra S. J Phy Soc Jpn 1992;61:1709.
[27] Hashmi SA, Kumar A, Maurya KK, Chandra S. J Phys D: Appl Phys 1990;23:1307.
[28] Sekhon SS, Kumar H. Bull Electrochem 1996;12:750.
[29] Sreekanth T, Jaipal Reddy M, Ramalingaiah S, Subba rao UV. J Power Sources 1999;79:105.
[30] Simmons JG. In: Maissel LI, Glang R, editors. Hand book of thin film technology. New York: Mc Graw-Hill; 1970.
[31] Ramu Ch, Naidu YRV, Sharma AK. Ferroelectrics 1994;159:275.
[32] Davis DS, Shalliday TS. Phys Rev 1960;118:1020.
[33] Thutupalli GM, Tomlin SG. J Phys D: Appl Phys 1976;9:1639.
[34] Frisch KC, Klempner D, Frisch HL. Polym Eng Sci 1998;22:1143.
[35] Bonardelli P, Moggi G, Turturro A. Polymer 1986;27:905.
[36] Utracki LA. Polymer alloys and blends. Munich: Hanser Publishers; 1989.